

Ultrahigh Harmonics from Laser-Assisted Ion-Atom Collisions

Manfred Lein and Jan M. Rost

Max Planck Institute for the Physics of Complex Systems, Nöthnitzer Straße 38, D-01187 Dresden, Germany
(Received 23 May 2003; published 8 December 2003)

We present a theoretical analysis of high-order harmonic generation from ion-atom collisions in the presence of linearly polarized intense laser pulses. Photons with frequencies significantly higher than in standard atomic high-harmonic generation are emitted. These harmonics are due to two different mechanisms: (i) collisional electron capture and subsequent laser-driven transfer of an electron between projectile and target atom; (ii) reflection of a laser-driven electron from the projectile leading to recombination at the parent atom.

DOI: 10.1103/PhysRevLett.91.243901

PACS numbers: 42.65.Ky, 32.80.Rm, 34.50.Rk, 34.70.+e

Over past decades, a vast amount of work has been devoted to the study of ion-atom collisions [1] and atoms in intense laser fields [2]. However, the two areas were almost entirely separated. No experiments on ion-atom collisions in the presence of strong laser pulses have been carried out. The reported experiments on laser-assisted collisions [3] involve one-photon processes and thermal collision energies. Also, theoretical descriptions [4] have mostly been limited to slow collisions and/or relatively weak fields. Recently, however, the theoretical works by Madsen *et al.* [5] and by Kirchner [6] investigate fast collisions in the presence of a strong laser field. In Ref. [5], excitation mechanisms are discussed, while Ref. [6] focuses on ionization and electron capture. In both cases, the field leads to a significant modification of the collision process. On the other hand, there has been no study on the question of how typical strong-field processes in atoms, such as high-order harmonic generation (HHG) [7] and above-threshold ionization [8], are modified due to the impact of an ion projectile. In HHG, a large number of incoming laser photons are converted into a single high-energy photon. HHG experiments are presently pursued with great effort [9] since the process serves as a source of coherent extreme ultraviolet radiation and attosecond pulses.

In the present work, we investigate HHG in a laser-assisted ion-atom collision. We focus on impact velocities such that the time scales of nuclear and electronic motion are comparable; i.e., we have significant probabilities for collisional electron transfer from the target to the projectile. For sufficiently long laser pulse durations, the laser-driven electron effectively sees a large range of internuclear distances during one laser pulse. When the laser polarization axis is parallel to the ion impact velocity, we show that this situation results in the generation of high harmonics with photon energies much higher than usually obtained in atomic HHG.

The recollision model [10] describes atomic HHG as a sequence of strong-field ionization, acceleration of the electron in the field, and recombination with the core. Within this model, the maximum return energy of the

electron is $3.17U_p$ where $U_p = E_0^2/(4\omega^2)$ is the ponderomotive potential for a laser with amplitude E_0 and frequency ω . The maximum energy of the emitted photon is then equal to $3.17U_p + I_p$ where I_p is the atomic ionization potential. For ion-atom collisions, we show below how the interplay between collisional electron capture and laser-driven electron transfer between target and projectile leads to new mechanisms of HHG with cutoffs at significantly higher energies.

We consider collisions of protons on hydrogen atoms for proton energies of 2 keV (impact velocity $v = 0.283$ a.u.). Because of the large impact momentum, the projectile trajectory is assumed to be classical and along a straight line. Furthermore, we use a two-dimensional model where all dynamics are restricted to the plane that contains the target nucleus and the projectile. The internuclear vector is $\mathbf{R}(t) = (X, Z) = (b, vt)$ where b is the impact parameter and v is the impact velocity. The interaction with the laser field $\mathbf{E}(t) = \mathbf{E}_0(t) \sin(\omega t + \delta)$ is treated in the dipole approximation and in velocity gauge. The time-dependent Hamiltonian then reads (atomic units are used throughout)

$$H(t) = \frac{\mathbf{p}^2}{2} + \mathbf{p} \cdot \mathbf{A}(t) + V(\mathbf{r}_t) + V(\mathbf{r}_p), \quad (1)$$

where $\mathbf{A}(t) = -\int_{-\infty}^t \mathbf{E}(t') dt'$, $\mathbf{r}_t = \mathbf{r} + \mathbf{R}(t)/2$, and $\mathbf{r}_p = \mathbf{r} - \mathbf{R}(t)/2$. For the electron-proton interaction V we use the soft-core potential from Ref. [11]. For the laser, we choose a wavelength of 800 nm and an intensity of 10^{14} W/cm². We use a trapezoidal pulse shape with a three-cycle turn on and turn off. The total pulse length τ is 16 optical cycles (42.7 fs).

Initially, the electron is in the ground state of the target atom, i.e., localized around $\mathbf{r}_t = 0$. The time-dependent Schrödinger equation is then solved numerically on a grid by means of the split-operator method [12] with 2048 time steps per cycle. The initial distance between target and projectile is set to $\mathbf{R}_0 = (b, -250$ a.u.) so that the closest approach occurs at midpulse. Until midpulse, the target atom is ionized with about 20% probability. Thus,

a significant fraction is retained for the interaction with the incoming proton. The HHG spectrum is calculated from the dipole acceleration $\langle \mathbf{a}(t) \rangle$ [13],

$$S(\omega) \sim \left| \int \langle \mathbf{a}(t) \rangle e^{i\omega t} dt \right|^2. \quad (2)$$

Figure 1 shows the harmonic spectrum obtained for a collision with impact parameter $b = 4$ a.u. and phase $\delta = 0$ of the laser. The two curves correspond to different directions of the laser polarization. If the polarization axis is perpendicular to the impact velocity, the emission spectrum has a form which is familiar from HHG in isolated atoms: a cutoff occurs at the photon energy $3.17U_p + I_p$. The slowly decreasing background for photon energies above 3 a.u. is due to numerical noise and can be lowered by reducing the time step and increasing the grid size. If the polarization axis is parallel to the impact velocity, the result is strikingly different. We find an extension of HHG to frequencies reaching slightly beyond $32U_p + I_p$. These structures are up to a factor of 10^5 more intense than the numerical background and remain stable as the numerical accuracy is improved. The region between $3.17U_p + I_p$ and $8U_p + I_p$ appears like an extension of the atomic plateau with a steeper slope. (The significance of the values $8U_p$ and $32U_p$ will be explained below.) Furthermore, interesting hump structures appear in the spectrum around 3, 5.6, and 6.6 a.u.

The inset of Fig. 1 shows the electric field $E(t)$ and the capture probability $P_{\text{cap}}(t)$ which we define as the probability that the electron is found within a square of size 40 a.u. \times 40 a.u. around the projectile. We see that the duration of the collisional capture is much shorter than the pulse length since electron capture is essentially an attosecond process; cf. [6]. After midpulse, P_{cap} decreases

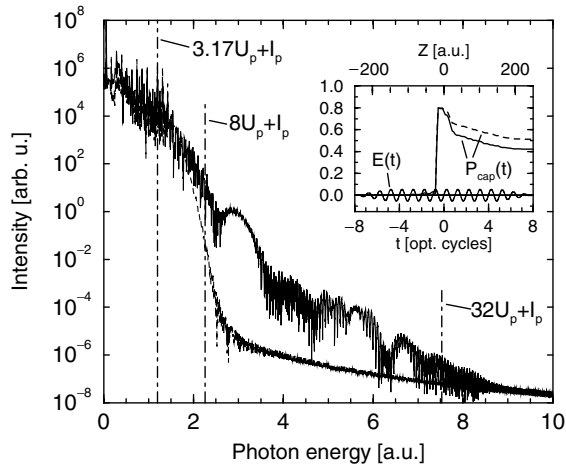


FIG. 1. Emission spectra for impact parameter $b = 4$ a.u. and laser phase $\delta = 0$. Upper curve (solid): polarization axis parallel to impact velocity. Lower curve (dashed): polarization axis perpendicular to impact velocity. The vertical lines indicate the cutoff energies for various mechanisms (see text). The inset shows the time dependence of the laser field and the capture probability for the two polarization directions.

due to laser-induced ionization. P_{cap} is smaller when the polarization is along the impact velocity, indicating more ionization during the collision.

Figure 2 gives a temporal analysis of the harmonic emission for the case that the laser is polarized parallel to the impact direction. Each spectrum in the figure is obtained by Fourier transforming the dipole acceleration over one laser cycle. Below the atomic cutoff, the emission is nearly independent of time, whereas there is initially no emission of ultrahigh harmonics ($Z = -140.5$ a.u.). Nevertheless, harmonics up to the highest frequency are produced already at $Z = -109.3$ a.u. and $Z = -78.1$ a.u., i.e., long before the actual ion-atom collision. Around $Z = 0$, the emission at the highest frequencies is weak. Instead, harmonics up to $8U_p + I_p$ are generated. At later times, emission at these energies drops, and, again, higher frequencies are produced. It is evident that the spectral structures at 3, 5.6, and 6.6 a.u. in Fig. 1 arise from emission around $Z = -46.8$ and -78.1 a.u.

As the next step, we vary the impact parameter b while keeping all other parameters constant. Figure 3(a) displays the final capture probability as a function of b , with and without laser field. Ionization reduces the capture probability significantly. The oscillatory behavior obtained as a function of b , however, is qualitatively unchanged.

Since we are particularly interested in harmonic generation well beyond the atomic cutoff, we define the yield of ultrahigh harmonics as the integrated quantity

$$S_{\text{uh}} = \int_{5U_p + I_p}^{\infty} S(\omega) d\omega. \quad (3)$$

The solid line in Fig. 3(b) displays the yield of ultrahigh harmonics versus b . Its overall structure is a monotonic decrease. A closer look reveals that the ‘‘dips’’ around

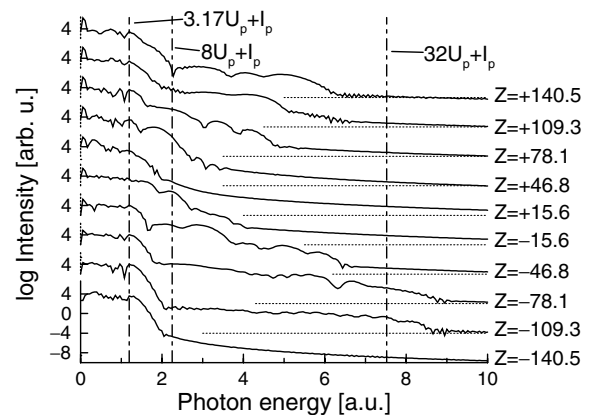


FIG. 2. Temporal analysis of harmonic emission for the same parameters as in Fig. 1. The polarization axis is parallel to the impact velocity. Each spectrum describes the emission during one laser cycle, and the value $Z = vt$ refers to the middle of the respective time interval. The dotted horizontal lines indicate the respective levels of $\log I = -10$.

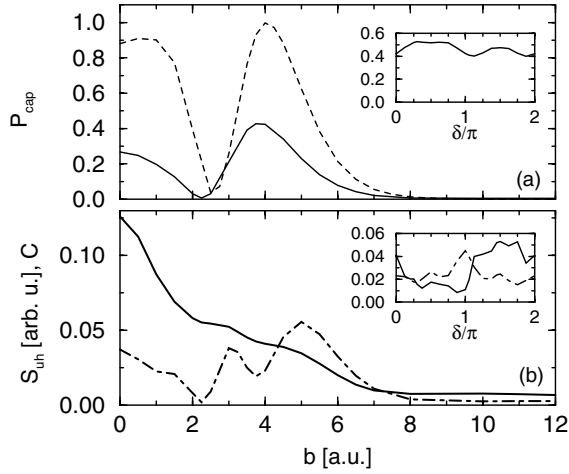


FIG. 3. (a) Solid curve: capture probability versus impact parameter b for a laser with phase $\delta = 0$; dashed curve: field-free capture probability. (b) Yield of ultrahigh harmonics (solid curve) and coherence parameter (dot-dashed curve) versus b . The polarization axis is parallel to the impact velocity. The insets show the same quantities as a function of the laser phase δ for fixed impact parameter $b = 4$ a.u.

$b = 2.5$ and 4 a.u. coincide with extrema of P_{cap} . For further investigation of this point we define the coherence parameter C according to $C = P_{\text{cap}}P_t$. Here, P_t is the final probability that the electron remains bound to the target atom, and is calculated analogous to P_{cap} . Small values of C indicate either ionization or localization of the electron at one of the two nuclei. For large values of C , the electron state is a coherent superposition of target and projectile states. Figure 3(b) shows that the maxima of C coincide with shoulders in S_{uh} while the minima in C coincide with the dips in S_{uh} .

We conclude that HHG beyond the atomic cutoff originates from at least two different mechanisms. One mechanism is unrelated to the coherence parameter and gives rise to the monotonic decreasing background in Fig. 3(b). Another mechanism depends on C and gives rise to the oscillations on top of the background.

The insets of Fig. 3 show the dependence on the laser phase δ for fixed impact parameter $b = 4$ a.u. As we vary δ , we find only modest changes in P_{cap} , but a significant alteration of S_{uh} . Phases between π and 2π give a higher yield than phases between 0 and π . No clear correlation with the coherence parameter C is observed, indicating that the mechanism unrelated to C dominates. This is consistent with the smallness of C at $b = 4$ a.u. We have not varied the initial internuclear distance since this is approximately equivalent to a change in δ .

It is beyond the scope of this work to investigate the question of phase matching between different impact parameters and laser phases. However, phase mismatch will not lead to a complete cancellation of harmonics but rather to a defocusing from the propagation axis.

As an explanation of our results, we propose the following two mechanisms. In mechanism (i), one of the

collision partners is ionized by the laser; the free electron is then accelerated in the field, and finally the electron recombines with the *other* ion. Mechanism (ii) also begins with the creation and acceleration of a free electron. Arriving at the other ion, the electron is elastically reflected and is further accelerated before it finally recombines with the core from which it was ejected.

Mechanism (i) has previously been suggested as a new mechanism of HHG in stretched molecules [14], and a cutoff at $8U_p + I_p$ was derived for the internuclear distances $R = (2n + 1)\pi\alpha$, $n = 0, 1, \dots$, where $\alpha = E_0/\omega^2$ is the classical quivering amplitude of the laser-driven electron. Until now, this cutoff has not been observed in experiment. A possible reason is that rather large internuclear distances are required. Moreover, the effect occurs only for systems where the electron state prior to ionization can be described by a single-particle orbital that is coherently delocalized over both nuclei. For example, this is a valid description for the ground state of H_2^+ , but not for a neutral molecule at large internuclear distances. In an ion-atom collision, a coherent superposition is realized if the coherence parameter C is appreciable. This explains the connection between C and S_{uh} in Fig. 3(b).

For fixed nuclei, we derive the maximum cutoff for both mechanisms from the classical electronic equation of motion, $\ddot{\mathbf{r}} = -\mathbf{E}_0 \sin\omega t$. For an electron starting with $\dot{\mathbf{r}} = 0$ at $\mathbf{r} = 0$ at time t_0 , we have

$$\dot{\mathbf{r}}(t) = (\mathbf{E}_0/\omega)(\cos\omega t - \cos\omega t_0). \quad (4)$$

Thus, the largest possible velocity equals $2E_0/\omega$, corresponding to $8U_p$ energy. If the field points along the internuclear distance, such an electron can recombine at the other ion and generate a photon with energy $8U_p + I_p$. This explains the cutoff law for mechanism (i). If the electron is instead elastically backscattered at time t_1 , the velocity is thereafter given by

$$\dot{\mathbf{r}}(t) = (\mathbf{E}_0/\omega)(\cos\omega t + \cos\omega t_0 - 2\cos\omega t_1), \quad t > t_1, \quad (5)$$

so that the maximum velocity is $4E_0/\omega$ corresponding to an energy of $32U_p$. A necessary condition for this maximum is that t_0 , t_1 , and t are times of zero electric field. By integrating Eq. (5) with the initial condition $\mathbf{r}(t_1) = \mathbf{R}$ and requiring $\mathbf{r}(t) = 0$, it is easy to show that recollision with the maximum energy is possible if the internuclear distance satisfies the condition $R = 3(2n + 1)\pi\alpha$, $n = 0, 1, \dots$. Therefore, at these distances we have a cutoff at $32U_p + I_p$. For the present laser parameters, $\alpha = 16.5$ a.u. and $U_p = 0.22$ a.u. Although nonzero ion velocities may lead to a correction of the cutoff, we conclude that the generation of ultrahigh harmonics (Figs. 1 and 2) is well explained by the reflection mechanism. With increasing ion velocity, we expect that the cutoff shifts towards higher energies since the electrons gain additional energy through the Fermi-shuttle mechanism

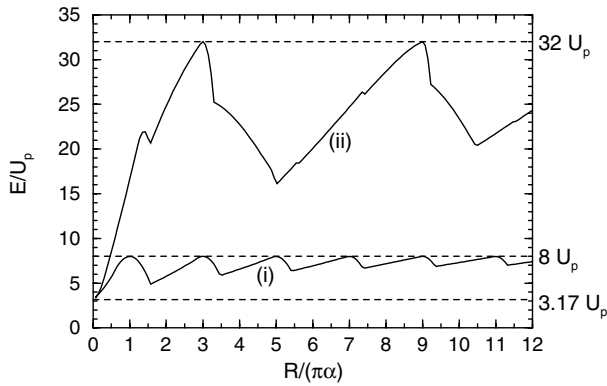


FIG. 4. Maximum classical kinetic energy versus internuclear distance for the recombination of a laser-driven electron in mechanisms (i) and (ii); see text (fixed-nuclei calculation).

[15]. Multiple reflections are in principle possible, but the signatures in the spectrum are negligible due to the small probability.

For mechanisms (i) and (ii), Fig. 4 shows the maximum electron energy at recombination time as a function of the internuclear distance. These results are obtained by numerical solution of the classical equation of motion for fixed nuclei. Both curves approach the atomic limit $3.17U_p$ for $R \rightarrow 0$. As expected, the maximum energies are found at $8U_p$ and $32U_p$.

The phase dependence in Fig. 3 is consistent with the reflection scenario. Before midpulse, reflection can occur only for electrons that are accelerated from the target towards the projectile. Under a phase shift by π , these electrons are accelerated in the opposite direction where they cannot be backscattered.

The discussed mechanisms should be a general feature of ion-atom collisions, and our results can be regarded as single-active-electron results for target atoms other than H, but with similar ionization potential. A disruption of coherent recollision by additional inner-electron capture in the multielectron case is unlikely at the large internuclear distances where most ultrahigh harmonics are generated.

A rough estimate shows that at least the lowest of the ultrahigh harmonics should be observable in an ion-atom collision experiment. Significant impact-factor weighted contributions come from $b \lesssim b_0 = 30$ a.u. Hence, a pulsed focused ion beam with $j = 10^{24}$ ions/s $^{-1}$ cm $^{-2}$ [16] gives rise to $N \approx j\tau b_0^2 \approx 10^{-3}$ hits per target atom during the laser pulse length τ . At photon energies around $8U_p + I_p$, the harmonic intensity in Fig. 1 is $p_{\text{uh}} \approx 10^{-4}$ below the plateau. The measurable ratio between ultrahigh and plateau signal is then $Np_{\text{uh}} \approx 10^{-7}$. Since plateau beam energies of $2\mu\text{J}$ have been achieved [17], we estimate an output of 2×10^4 photons which is well above the lower detection limit of less than 100 photons [18].

Furthermore, the proposed mechanisms are expected to play an important role in a variety of situations where

laser-driven electrons can interact with nearby particles, e.g., HHG in exploding clusters and in large molecules or HHG from atoms near surfaces. Note that an extension of the HHG plateau has been observed in Ar clusters [19].

In summary, we have investigated ion-atom collisions in a strong laser field. Harmonics with energies much larger than in atomic HHG are generated if the laser polarization is parallel to the direction of impact. We have proposed two distinct HHG mechanisms, involving laser-driven transfer of electrons between the collision partners. The highest harmonics are due to reflection of electrons from the projectile back to the target atom at times of large projectile-target distances. A simplified classical description gives a cutoff at $32U_p + I_p$ for this process.

-
- [1] R. Dörner *et al.*, Phys. Rep. **330**, 95 (2001).
 - [2] M. Protopapas, C. H. Keitel, and P. L. Knight, Rep. Prog. Phys. **60**, 389 (1997); P. Lambropoulos, P. Maragakis, and J. Zhang, Phys. Rep. **305**, 203 (1998).
 - [3] A. Débarre and P. Cahuzac, J. Phys. B **19**, 3965 (1986).
 - [4] G. Ferrante, L. L. Cascio, and B. Spagnolo, J. Phys. B **14**, 3961 (1981); T. S. Ho, C. Laughlin, and S.-I. Chu, Phys. Rev. A **32**, 122 (1985); Y. P. Hsu and R. E. Olson, Phys. Rev. A **32**, 2707 (1985); C. Chaudhuri and T. K. Rai Dastidar, Nuovo Cimento D **20**, 749 (1998); A. B. Voitkiv and J. Ullrich, J. Phys. B **34**, 1673 (2001); S.-M. Li, J. Chen, and Z.-F. Zhou, J. Phys. B **35**, 557 (2002).
 - [5] L. B. Madsen, J. P. Hansen, and L. Kocbach, Phys. Rev. Lett. **89**, 093202 (2002).
 - [6] T. Kirchner, Phys. Rev. Lett. **89**, 093203 (2002).
 - [7] A. McPherson *et al.*, J. Opt. Soc. Am. B **4**, 595 (1987).
 - [8] P. Agostini, F. Fabre, G. Mainfray, G. Petite, and N. K. Rahman, Phys. Rev. Lett. **42**, 1127 (1979); J. H. Eberly, J. Javanainen, and K. Rzażewski, Phys. Rep. **204**, 331 (1991).
 - [9] C. Spielmann *et al.*, Science **278**, 661 (1997); A. Paul *et al.*, Nature (London) **421**, 51 (2003).
 - [10] P. B. Corkum, Phys. Rev. Lett. **71**, 1994 (1993).
 - [11] M. Protopapas, D. G. Lappas, and P. L. Knight, Phys. Rev. Lett. **79**, 4550 (1997).
 - [12] M. D. Feit, J. A. Fleck, Jr., and A. Steiger, J. Comput. Phys. **47**, 412 (1982).
 - [13] K. Burnett, V. C. Reed, J. Cooper, and P. L. Knight, Phys. Rev. A **45**, 3347 (1992).
 - [14] P. Moreno, L. Plaja, and L. Roso, Phys. Rev. A **55**, R1593 (1997); A. D. Bandrauk, S. Chelkowski, H. Yu, and E. Constant, Phys. Rev. A **56**, R2537 (1997); R. Kopold, W. Becker, and M. Kleber, Phys. Rev. A **58**, 4022 (1998).
 - [15] E. Fermi, Phys. Rev. **75**, 1169 (1949).
 - [16] W. Schimassek, W. Bauer, and O. Stoltz, Rev. Sci. Instrum. **62**, 168 (1991).
 - [17] J.-F. Hergott *et al.*, Phys. Rev. A **66**, 021801(R) (2002).
 - [18] L. Poletto, G. Tondello, and P. Villorresi, Rev. Sci. Instrum. **72**, 2868 (2001).
 - [19] T. D. Donnelly, T. Ditmire, K. Neuman, M. D. Perry, and R. W. Falcone, Phys. Rev. Lett. **76**, 2472 (1996).